Postprint of Carbide Evolution Behavior in High-Tungsten K416B Cast Nickel-Based Alloy During High-Temperature Creep

Authors: Xie Jun, Yu Jinjiang, Sun Xiaofeng, Jin Tao

Date: 2016-11-04T00:00:00+00:00

Abstract

Through creep performance testing and microstructural morphology observation, the evolution behavior of precipitated phases in high-tungsten K416B nickel-based alloy during high-temperature creep was investigated. The results show that in the as-cast alloy, the γ' phase exhibits size inhomogeneity, and rod-like MC carbides are distributed in a Chinese-character-shaped pattern within interdendritic regions. During high-temperature creep under applied stress, fine M6C carbides can precipitate discontinuously in the deformed matrix. Thermodynamic analysis indicates that under stress-induced conditions, element C segregates at stress concentration sites and combines with carbide-forming elements such as W, thereby promoting the precipitation of fine M6C phase from the matrix. Concurrently, grooves form on the surfaces of rod-like MC carbides, which gradually decompose and transform into granular M6C phase. The additional stress generated on the surface of rod-like MC phase constitutes the primary mechanism for the continuous dissolution and spheroidization of MC phase.

Full Text

CARBIDE EVOLUTION BEHAVIOR OF K416B AS-CAST Ni-BASED SUPERALLOY WITH HIGH W CONTENT DURING HIGH TEMPERATURE CREEP

XIE Jun, YU Jinjiang, SUN Xiaofeng, JIN Tao, SUN Yuan

Institute of Metal Research, Chinese Academy of Sciences, Shenyang 110016

Correspondent: Yu Jinjiang, professor, Tel: (024)23971713, E-mail: jjyu@imr.ac.cn

Supported by National Basic Research Program of China (Nos. 2010CB631200 and 2010CB631206) and National Natural Science Foundation of China (No. 50931004)

Manuscript received 2014-10-08, in revised form 2014-12-22

ABSTRACT

As-cast Ni-based superalloys with high W content are used extensively in turbine vanes of aero-engines due to their good oxidation resistance and temperature capability. During high temperature service, creep deformation and microstructure evolution occur in these materials, and the creep behavior mainly depends on their chemical composition and microstructure, such as the size, distribution, and morphology of the γ phase and carbides. Among these, the morphologies of carbide phases are closely related to the creep resistance of the alloy. Generally, carbide particles displaying dispersive distribution may enhance creep resistance, while carbides with continuous morphologies distributed at boundaries may provide easy paths for crack propagation and degrade the mechanical properties. Besides, the creep life of the alloy also depends on microstructure evolution at high temperature. However, the evolution mechanism of carbides in K416B superalloy during creep remains unclear. For this reason, by means of creep property measurement and microstructure observation, the evolution behavior of precipitates in K416B Ni-based superalloy with high W content during high temperature creep has been investigated. The results show that the size of the γ phase is inhomogeneous in the as-cast alloy, and stripe MC carbides distribute in inter-dendritic regions displaying Chinese character-like structures. During high temperature creep under applied stress, fine M6C carbides discontinuously precipitate in the deformed γ matrix. Thermodynamic analysis indicates that carbon element segregates in regions of stress concentration and combines with carbide-forming elements such as W, which promotes the precipitation of fine M6C carbides from the γ matrix. At the same time, grooves are formed on the surface of stripe MC carbides, which then gradually decompose and transform into M6C particles. The additional stress formed on the surface of stripe MC carbides is the main factor promoting continuous dissolution and spheroidization of the MC phase.

KEY WORDS K416B Ni-based superalloy, creep, carbide evolution, thermodynamics analysis

1. Introduction

Ni-based cast superalloys with high tungsten content are considered important materials for manufacturing aero-engine turbine guide vanes due to their excellent oxidation resistance and temperature capability [1-3]. The K416B Ni-based superalloy contains W up to 16.3 wt% and exhibits good thermal fatigue performance, making it one of the equiaxed cast superalloys with higher temperature-bearing capacity [4]. Tungsten is an important solid solution el-

ement in Ni-based superalloys, with a partition ratio of approximately 1:1 in both γ and γ phases, which can simultaneously strengthen both phases and improve creep strength [5-7]. Additionally, W is a primary element for carbide formation and can form various types and morphologies of carbides during solidification [8,9], directly affecting the mechanical properties of the alloy. Studies on high-W M963 alloy [10,11] have shown that as the melt processing temperature increases, carbide morphology transforms from blocky to Chinese character-like to granular, with more uniform carbide distribution that can improve the alloy' s stress rupture properties. During high temperature thermal exposure, carbides in Ni-Cr-W alloys can undergo decomposition reactions (M6C $\rightarrow$ M23C6 + M (W, Ni, Cr, Mo)), with M23C6 carbides precipitating along grain boundaries while maintaining certain orientation relationships with the matrix [12,13]. Furthermore, related studies [14-16] have shown that after long-term aging, carbides in cast Ni-based alloys can undergo the transformation: MC + $\gamma \rightarrow$ + M23C6(M6C), and with increasing aging temperature and time, the amount of secondary M23C6(M6C) carbides increases.

During high temperature service of Ni-based superalloys, microstructural evolution occurs, mainly including coarsening and rafting of the γ phase, degeneration of carbides (such as MC $\rightarrow$ M23C6 or M6C), and secondary precipitation of strengthening phases (γ phase and carbides) [17,18]. This evolution is closely related to the service life of the alloy. Therefore, studying microstructural evolution and related mechanisms during high temperature creep is important for predicting alloy service life [19]. For high-W K416B alloy, the microstructure mainly consists of γ phase, γ phase, and carbides. During high temperature creep, creep deformation inevitably occurs accompanied by transformation of precipitates, but the carbide evolution mechanism in high-W alloys during high temperature creep remains unclear.

In this work, creep property tests were conducted on high-W K416B alloy, and microstructural observations were performed using scanning electron microscopy (SEM) and transmission electron microscopy (TEM) to investigate the evolution mechanism of precipitates during high temperature creep, aiming to provide a theoretical basis for alloy development and application.

The K416B master alloy ingot was remelted in a 10 kg vacuum induction furnace and cast into equiaxed crystal bars. The nominal composition of the alloy (wt%) is: C 0.13, Cr 4.90, Co 6.82, Nb 2.06, Al 5.75, W 16.3, Ti 1.00, Hf 1.00, Ni balance. The alloy bars were machined into cylindrical specimens with a gauge length of 25 mm and diameter of 5 mm. The specimens were placed in an F-25 creep/stress rupture testing machine and subjected to creep tests at 1000 ℃ under an applied stress of 150 MPa for different durations.

The crept specimens were ground and polished, then chemically etched using a solution of 20 mL HCl + 5 g CuSO4 + 25 mL H2O. Microstructural observations were conducted using an S-3400N SEM, and energy dispersive spectroscopy (EDS) was performed on precipitates in the alloy. Thin slices of 0.5 mm thickness were cut from the crept specimens using wire electrical discharge machining,

mechanically ground on both sides to 50 m, and punched into 3 mm diameter discs. TEM samples were prepared by twin-jet electropolishing at -25 ℃ using a 10% perchloric acid alcohol solution. A TECNAI-20 TEM was then used to observe the microstructure of the crept and fractured alloy.

2. Experimental Results

The creep curve of K416B alloy at 1000 ℃ under an applied stress of 150 MPa is shown in Figure 1 [FIGURE:1]. The alloy exhibits a low steady-state creep rate of approximately 0.00716 %/h, with a steady-state duration of about 120 h. The creep life reaches 154 h, and the post-fracture elongation is 4.7%.

The microstructure of as-cast K416B alloy is shown in Figure 2

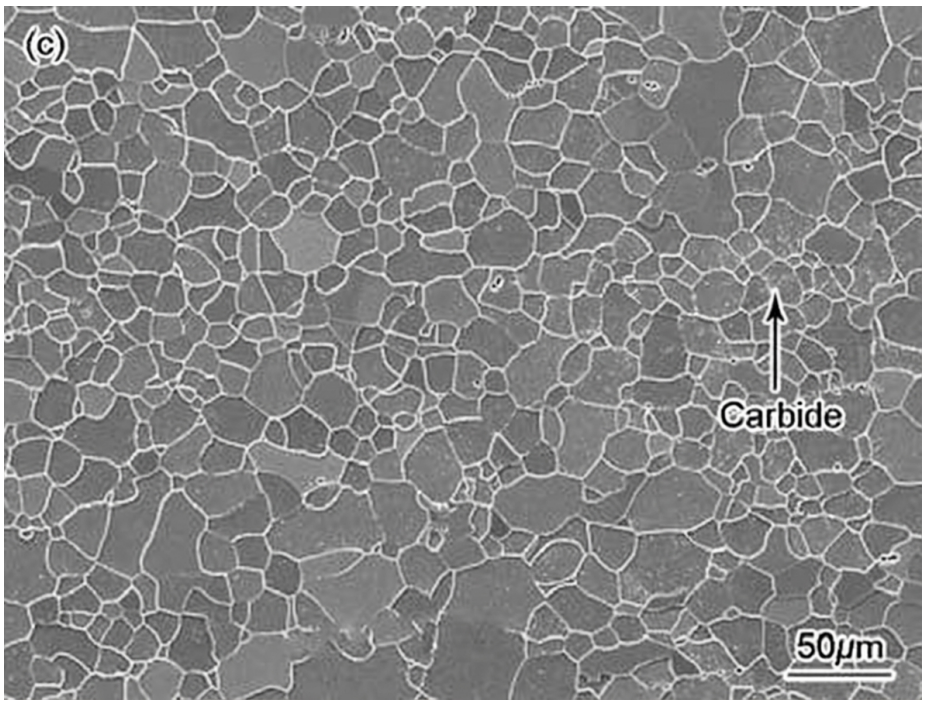

Figure 1: Figure 2

. The γ phase exhibits non-uniform size distribution, with larger γ phases (1-2 m) in inter-dendritic regions showing irregular distribution (upper right in Figure 2a), while smaller γ phases (0.3-0.6 m) are present in dendrite cores (lower left in Figure 2a). Figure 2b shows the morphology of carbides in the as-cast alloy, where stripe-like MC carbides with straight surfaces are observed to distribute in inter-dendritic regions in a Chinese character-like pattern.

The microstructures of the alloy after creep for different times at 1000 ℃ under

150 MPa are shown in Figure 3 [FIGURE:3], where creep times of 5, 50, and 145 h correspond to the primary, secondary, and tertiary creep stages, respectively. After 5 h of creep, the γ phase in inter-dendritic regions shows slight coarsening with small deformation, and only a few white particles precipitate (Figure 3a). After 50 h of creep, the coarsening of γ phase becomes more evident, forming rafted structures, and the number of fine white particles increases (Figure 3b). The microstructure after creep fracture is shown in Figure 3c, where the rafted γ structure becomes distorted and irregularly distributed, and the number of fine white particles further increases. EDS analysis indicates that these fine particles are rich in W, Cr, and C. This demonstrates that as creep progresses, the γ phase coarsens, and compared with the as-cast microstructure (Figure 2a), numerous fine white particles precipitate dispersively in the deformed matrix.

The evolution morphology of stripe carbides in inter-dendritic regions during creep at 1000 ℃ under 150 MPa is shown in Figure 4 [FIGURE:4]. After 5 h of creep, grooves form on the surface of stripe carbides, showing an uneven characteristic (Figure 4a). After 50 h of creep, the grooves on the carbide surface deepen (Figure 4b), and local regions of the stripe carbides fuse to form granular particles. After creep fracture, the stripe carbides are broken into granular particles distributed discontinuously (Figure 4c). This indicates that during high temperature creep, stripe carbides are gradually fused into discontinuously distributed granular phases.

TEM images of stripe carbides in K416B alloy during creep at 1000 ℃ under 150 MPa are shown in Figure 5 [FIGURE:5]. After 50 h of creep, the stripe carbide surface appears uneven, and a few slip dislocations terminate at the carbide, indicating that stripe carbides can effectively hinder dislocation motion. EDS analysis of this stripe carbide shows it is rich in Nb, W, Hf, Ti, and C elements. The corresponding selected area electron diffraction (SAED) pattern is shown in the inset of Figure 5a, confirming the stripe phase as MC-type carbide.

Figure 5b shows a TEM image of fused stripe carbides in the crept and fractured K416B alloy. Clear grooves formed by dissolution can be observed on the carbide surface, with numerous dislocation traces near the grooves. The fused carbides appear granular. EDS analysis indicates these granular particles are rich in W, Nb, Cr, and C. The SAED pattern in the inset of Figure 5b identifies these particles as M6C-type carbides. Analysis suggests that during high temperature creep, stripe MC-type carbides in inter-dendritic regions can fuse and transform into granular M6C-type carbides.

Figure 6 [FIGURE:6] shows the microstructure of K416B alloy after creep fracture at 1000 ℃ under 150 MPa for 154 h. Fine granular carbides precipitate dispersively at dislocation pile-up regions and γ/γ interfaces in the matrix. The SAED pattern in the inset of Figure 6a confirms these precipitates as M6C-type carbides, with numerous deformation dislocations tangled near the fine carbides. In another local region of the crept and fractured alloy, fused carbides distribute in a chain-like pattern, with mobile dislocations piled up near the granular carbides. This indicates that both secondary fine carbides precipitated during

creep and fused granular carbides can effectively hinder dislocation motion and improve creep resistance.

3.1 Stress-Induced Precipitation of Fine Carbides

During steady-state creep of K416B alloy at 1000 ℃ under 150 MPa, the strain rate is low (0.00716 %/h). As creep progresses, because the γ phase is stronger than the γ matrix, the matrix deforms more than the γ phase, leading to a gradual increase in dislocation density in the matrix and resulting in stress concentration and high flow stress at interfaces. This provides favorable conditions for fine carbide precipitation in the matrix and promotes the dispersive precipitation of M6C phase from the deformed alloy (Figure 6a), indicating that stress induction during creep can cause fine carbides to precipitate from the matrix.

The stress-induced precipitation of fine carbides from the matrix can be analyzed using phase equilibrium thermodynamics theory. Since the as-cast K416B alloy contains high W content (16.3%) and no fine carbides precipitate in the matrix in the as-cast condition (Figure 2a), the carbon in the matrix is in equilibrium, providing necessary conditions for M6C carbide precipitation. During creep, the alloy matrix undergoes plastic deformation, and the applied stress and thermal deformation increase the chemical potential of carbon in the γ matrix, making it supersaturated. Additionally, crystal slip and plastic deformation release deformation heat, which can cause fine M6C carbides to precipitate in the γ matrix. The effect of applied stress on the solubility of carbon in the γ matrix can be analyzed according to thermodynamic theory regarding the effect of applied stress on phase equilibrium [20]. The relationship describing how applied stress affects carbon solubility in the γ matrix can be expressed as:

Where is the mole fraction of solute C dissolved in the γ phase, is the mole fraction of solute C in M6C-type carbides, is the molar volume of M6C carbides, and is the Gibbs free energy.

Since the composition difference between the γ phase and MC-type carbides is large, ( ) can be considered constant. Applying the regular solution model [21] to the γ phase and performing corresponding approximations yields the following equation:

Where and are the mole fractions of solute C dissolved in the γ phase without and with applied stress, respectively; σ is the applied stress; R is the gas constant; and T is the thermodynamic temperature. Equation (2) shows that applied stress affects the solubility of solute C in the γ phase. When tensile stress is applied during creep, σ is negative, making ( ) < 1, which indicates that applied tensile stress during creep reduces the solubility of solute C in the γ phase. During creep under applied tensile stress, as dislocation density in the matrix increases, deformation heat is released while solute C segregates at stress concentration sites. Additionally, due to its small atomic radius and thermodynamic activity for carbide formation, C can combine with strong carbide-forming

elements such as W and Cr, promoting discontinuous precipitation of solute C as carbides in the matrix or at γ/γ interfaces.

3.2 Analysis of Stripe Carbide Evolution Mechanism

EDS analysis shows that elements Nb, W, Hf, and Ti are the main constituents of stripe MC-type carbides, while fused M6C-type carbides are rich in W, Nb, and Cr. The elements that promote carbide formation are collectively referred to as T elements. Since both MC and M6C carbides have fcc structures, stripe MC carbides can fuse and transform into secondary M6C phase during high temperature creep under applied stress (Figure 5). The transformation reaction [22] can be expressed as:

The fusion process of stripe MC carbides can be analyzed using equilibrium thermodynamics theory. During creep, because stripe carbides can effectively hinder dislocation motion (Figure 5), stress concentration easily forms, creating additional stress PMC/γ on their surfaces. Combining with Equation (2), we can derive:

Where and are the molar concentrations of T elements in MC phase and γ phase, respectively, and is the molar volume of MC carbides. As creep progresses and matrix deformation increases, the additional stress on the stripe MC phase surface increases, raising the concentration of T elements in the adjacent γ phase and causing T elements to diffuse from the MC phase into the γ matrix, thus accelerating the decomposition of stripe MC phase.

During creep, the additional stress (PMC/γ) generated by applied stress at the stripe MC/γ two-phase interface significantly affects the equilibrium concentration of T elements in the MC/γ phases, causing grooves to appear on the stripe MC carbide surface until fusion and spheroidization occur. The effect of this additional stress on the fusion and spheroidization of stripe MC phase is schematically shown in Figure 7 [FIGURE:7]. In as-cast K416B alloy, stripe MC phase has a smooth surface. During high temperature creep under applied stress, additional stress is generated at the MC/γ interface (Figure 7a). Under applied stress during high temperature creep, stripe MC phase decomposes to form grooves under the action of additional stress, with interface tension produced with the adjacent γ phase as shown in Figure 7b. At the groove intersection, the instantaneous equilibrium relationship between the interface tension of two MC phases with the γ matrix and the additional stress (PMC/γ) can be expressed as:

Where is the interface tension formed by MC phase decomposition creating grooves with the adjacent γ phase, and α is the included angle of grooves formed by MC phase decomposition. As creep further progresses, under the action of additional stress, T elements continuously diffuse from the MC phase to the adjacent γ phase at groove locations, making it a high-concentration region of T elements. Subsequently, T elements diffuse from high-concentration to low-concentration regions in the γ phase, and some T elements diffuse from the

γ matrix into stripe MC phase, gradually transforming stripe MC phase into granular M6C phase (Figure 7c), causing the interface tension at groove intersections to lose equilibrium. To maintain equilibrium, the curved front of granular M6C phase continuously dissolves. Therefore, during the transformation and spheroidization of MC phase to M6C phase, the relationship of interface tension at its curved front should be:

Thus, it can be concluded that the additional stress (PMC/γ) generated on the stripe MC surface during creep is the main factor causing continuous deepening of MC phase grooves and decomposition of MC phase. In other words, under the combined action of strain energy and interface energy, element diffusion occurs, gradually deepening grooves and increasing thickness of MC phase, leading to decomposition and transformation of adjacent MC phases into granular M6C phase.

3.3 Effect of Microstructural Evolution Characteristics on Creep Properties of High-W Superalloy

During high temperature creep under applied stress, fine M6C carbides can precipitate dispersively under stress induction at dislocation pile-up regions and γ/γ interfaces. As creep progresses, the number of fine M6C precipitates gradually increases (Figure 3), and the precipitated fine M6C carbides can effectively hinder dislocation motion (Figure 6a). The strengthening effect [23] can be expressed as:

Where $\Delta\tau$s is the strengthening effect of precipitated fine carbides, r is the average radius of fine carbide particles, f is the volume fraction of precipitated fine carbides, and and k are material-related constants. This shows that as creep progresses and the number of fine M6C carbides increases (i.e., f increases), the creep resistance of the alloy improves, which is one of the main reasons for the low steady-state strain rate of the alloy.

Related studies [24,25] have shown that during creep under applied stress, deformation dislocations easily pile up at stripe-like phases in the alloy, creating stress concentration. When the concentrated stress exceeds the bonding strength between the stripe-like phase and the matrix, cracks initiate and propagate along their interface, accelerating alloy fracture, which is considered a weak link during creep. In contrast, granular phase regions are less prone to stress concentration and can provide dispersion strengthening, improving alloy strength [26]. Therefore, the fusion of stripe MC-type carbides into granular M6C carbides during high temperature creep in K416B alloy is beneficial for relieving stress concentration generated during creep and improving creep strength, thus extending the steady-state duration of K416B alloy.

4. Conclusions

(1) In as-cast K416B alloy, the γ phase shows non-uniform size distribution in inter-dendritic and dendrite core regions with irregular morphology, and stripe MC carbides distribute in inter-dendritic regions in a Chinese character-like pattern.

(2) During high temperature creep, fine granular M6C carbides precipitate dispersively under stress induction. Analysis suggests that applied stress reduces the solubility of C element in the γ matrix, causing it to segregate at stress concentration sites and combine with carbide-forming elements such as W, promoting discontinuous precipitation of fine M6C phase from the matrix and γ/γ interfaces.

(3) During high temperature creep under applied stress, stripe MC carbides coarsen, develop uneven surfaces, and gradually dissolve and transform into granular M6C phase. The additional stress formed on the surface of stripe MC carbides is the main factor promoting continuous decomposition and spheroidization of MC phase.

References

[1] Liu Y, Hu R, Li J S, Kou H C, Li H W, Chang H, Fu H Z. Mater Sci Eng, 2009; A508: 141 [2] Kim I S, Choi B G, Hong H U, Do J, Jo C Y. Mater Sci Eng, 2014; A593: 55 [3] Zhang G Q. Acta Metall Sin (Engl Lett), 2005; 18: 55 [4] Yang Y H, Yu J J, Sun X F, Jin T, Guan H R, Hu Z Q. Mater Des, 2012; 36: 699 [5] Tang B, Jiang L, Hu R, Li Q. Mater Charact, 2013; 78: 144 [6] Zheng Y R, Xie J Z. Journal of Aeronautical Materials, 2009; 29(6): 1 [7] Qin X Z, Guo J T, Yuan C, Hou J S, Ye H Q, Mater Lett, 2008; 62: 2275 [8] Hou J S, Guo J T, Wu Y X, Zhou L Z, Ye H Q. Mater Sci Eng, 2010; A527: 1548 [9] Zheng L, Gu C Q, Zeng Q, Hou S E. Journal of Aeronautical Materials, 2004; 24(1): 17 [10] He L Z, Sun X F, Zheng Q, Hou G C, Zhang C Z, Guan H R, Hu Z Q. Materials Engineering, 2004; (2): 40 [11] Yuan C, Sun X F, Yin F S, Guan H R, Hu Z Q, Zheng Q, Yu Y. J Mater Sci Technol, 2001; 17: 425 [12] Bai G H, Li J S, Hu R, Zhang T B, Kou H C, Fu H Z. Mater Sci Eng, 2011; A528: 2339 [13] Yang J X, Zheng Q, Sun X F, Guan H R, Hu Z Q. Mater Sci Eng, 2007; A465, 100 [14] Qin X Z, Guo J T, Yuan C, Hou J S, Ye H Q. Mater Sci Forum, 2007; 546-549:1301 [15] Yang J X, Sun Y, Jin T, Sun X F, Hu Z Q. Acta Metallurgica Sinica, 2014; 50: 839 [16] Xiao X, Zeng C, Hou J S, Qin X Z, Guo J T, Zhou L Z. Acta Metallurgica Sinica, 2014, 50: 1031 [17] Wang L, Wang S, Song X, Liu Y, Xu G H. Int J Fatigue, 2014; 62: 210 [18] Yang J X, Zheng Q, Sun X F, Guan H R, Hu Z Q. Mater Sci Eng, 2006; A429: 341 [19] Seo S M, Kim I S, Lee J H, Jo C Y, Miyahara H, Ogi K. J Met Sci Technol, 2008; 24: 110 [20] Mats H, translated by Lai H Y, Liu G X. Alloy Diffusion and Thermodynamics. Beijing: Metallurgical Industry Press, 1984: 103 [21] Mats H, Translated by Li Q B, Wang X C. Diffusion Controlled Reactions in Alloy and Thermodynamic of Alloy. Shenyang: Liaoning Science and Technology Press, 1984: 204 [22] Lvov

G, Levit V I, Kaufman M J. Metall Mater Trans, 2004; A35: 1669 [23] Mao W M, Zhu J C, Li J, Long Y, Fan Q C. The Structure and Properties of Metallic Materials. Beijing: Tsinghua University Press, 2008: 186 [24] Tian S G, Wang M G, Li T, Qian B J, Xie J. Mater Sci Eng, 2010; A527: 5444 [25] Xie J, Tian S G, Zhou X M, Yu X F, Wang W X. Mater Sci Eng, 2012; A538: 306 [26] He L Z, Zheng Q, Sun X F, Guan H R, Hu Z Q, Tieu A K, Lu C, Zhu H T. Metall Mater Trans, 2005; A36: